https://doi.org/10.5194/egusphere-2026-3400
Preprint. Discussion started: 1 July 2026

Behavior of aerosol particles during dust- and pollen-affected time periods in southern Finland

Sujai Banerji[1], Touqeer Gill[1], Veli-Matti Kerminen[1], and Tuukka Petäjä[1]

[1]Institute for Atmospheric and Earth System Research (INAR)/Physics, Faculty of Science, University of Helsinki, Helsinki, Finland

Correspondence: Sujai Banerji (sujai.banerji@helsinki.fi) and Tuukka Petäjä (tuukka.petaja@helsinki.fi)

Abstract. Natural dust and pollen episodes can alter aerosol particles, meaning tiny particles suspended in air, but their effects are not always easy to distinguish from optical measurements alone. We studied dust- and pollen-affected time periods at the Station for Measuring Ecosystem–Atmosphere Relations II (SMEAR II), a boreal forest field station in Hyytiälä, southern Finland. We combined in situ measurements of aerosol light scattering and absorption, size-resolved particulate matter mass, and aerosol particle size distributions. The merged optical and mass dataset contained 36 labelled event-affected sampling intervals: 15 dust-affected and 21 pollen-positive intervals. A separate event-level sensitivity analysis grouped the higher-resolution size-distribution data into 23 temporally separated episodes: 15 dust and 8 pollen episodes. Both dust- and pollen-affected periods increased aerosol scattering, showing that an optical enhancement can indicate that an atmospheric event occurred. However, bulk optical properties overlapped strongly and did not reliably identify whether the event was dust or pollen. Size-resolved mass and particle size-distribution measurements provided clearer physical information. Event–background differences increased with particle size and were strongest for particles larger than 10 micrometres, while accumulation-mode particle surface area showed the clearest temporally controlled dust–pollen tendency. These results show that, at this boreal forest site, dust and pollen can produce similar optical responses but different size-resolved particle responses. The study therefore helps clarify how long-term aerosol observations should be interpreted, and it cautions against assigning source type from optical enhancement alone. These findings support cautious use of monitoring records in boreal and other background environments.

1 Introduction

Mineral dust and pollen episodically modify atmospheric aerosol populations by adding particles and changing particle-size distributions, particulate matter (PM) mass, and optical properties. At SMEAR II (Station for Measuring Ecosystem–Atmosphere Relations II), the Hyytiälä boreal forest station in southern Finland, these perturbations occur within a boreal background shaped by new-particle formation, biogenic emissions, meteorology, transport, and long-term variability in aerosol composition and optics (Banerji et al., 2025; Buenrostro Mazon et al., 2009; Dal Maso et al., 2005; Heikkinen et al., 2020; Luoma et al., 2019).

https://doi.org/10.5194/egusphere-2026-3400
Preprint. Discussion started: 1 July 2026

Dust and pollen differ in source process, transport pathway, morphology, composition, and size distribution. Nevertheless, their receptor-site optical responses can overlap. Both event types can increase supermicron particle abundance, scattering, and PM mass. Long-range transported dust has been documented over Finland, and pollen can contribute optically detectable depolarizing particles (Bohlmann et al., 2019, 2021; Meinander et al., 2023; Varga et al., 2023). However, in-situ scattering and scattering Ångström exponent (SAE) are not source-specific because they depend on particle loading, size distribution, refractive index, hygroscopicity, and mixing state (Schuster et al., 2006; Seinfeld and Pandis, 2016; Titos et al., 2021).

The central question is therefore not only whether an aerosol event occurred, but whether the measured variables contain source-type information. We distinguish three related tasks. The overall event response describes how dust- and pollen-affected periods modify the aerosol population. Event detection tests whether dust- or pollen-affected observations differ from non-event background conditions. Event typing tests whether dust-affected observations differ from pollen-positive observations within the labelled event subset. These terms are used retrospectively for already labelled observations; they do not imply a forecasting model, a real-time source classifier, or a prediction mechanism.

A retrospective non-parametric effect-size framework is useful because the event labels are operational, the dust and pollen evidence streams differ, event counts are small and unequal, aerosol variables are often skewed, and repeated measurements within one atmospheric episode are temporally dependent. The framework emphasizes effect direction, effect size relative to background variability, confidence-interval width, consistency across temporal corrections, and stability under event-level sensitivity checks. This keeps the interpretation close to the observational evidence and avoids presenting the analysis as a source-classification method.

Two event counts are therefore used in this manuscript, and they refer to different observational units. The merged optical–PM-mass analysis uses 36 labelled 2–3 d cascade-impactor sampling intervals, consisting of 15 dust-affected and 21 pollen-positive intervals. The APSD event-level sensitivity analysis starts from native-resolution size-distribution observations and then declusters them into 23 temporally separated episodes, consisting of 15 dust and 8 pollen episodes under the primary 48 h rule. The 23-episode count is used to reduce temporal dependence in the APSD robustness checks; it does not replace the 36 labelled sampling intervals used in the merged optical–PM-mass analysis.

The present study was therefore guided by three research objectives:

1. Quantify how dust- and pollen-affected time periods modify aerosol optical properties, aerosol particle size distributions, and PM-mass concentrations at SMEAR II.

2. Identify variables derived from in-situ aerosol observations that show statistically distinguishable and physically interpretable differences between non-event background conditions and dust- or pollen-affected conditions.

3. Refine the screened event-responsive variables by identifying which ones also show a statistically distinguishable and physically interpretable contrast between dust-affected and pollen-positive observations.

We first compare labelled event-affected observations with the non-event background. We then test whether the event-responsive variables also distinguish dust-affected from pollen-positive observations. Finally, we use size-distribution

https://doi.org/10.5194/egusphere-2026-3400
Preprint. Discussion started: 1 July 2026

information to interpret why bulk optical properties can overlap even when size-resolved mass and accumulation-mode aerosol particle size-distribution metrics show clearer event-type tendencies.

2 Materials and Methods

2.1 Study site and measurement datasets

Aerosol optical, PM-mass, and particle size-distribution measurements from SMEAR II, Hyytiälä, southern Finland, were analysed under background, pollen-positive, and dust-affected conditions (Banerji et al., 2025; Hari and Kulmala, 2005; Luoma et al., 2019). SMEAR II is a long-term field station for ecosystem–atmosphere and atmospheric-composition measurements, including continuous aerosol, trace-gas, meteorological, and forest-environment observations. The optical and PM-mass measurements follow the SMEAR II supermicron aerosol measurement framework described by Banerji et al. (2025). Briefly, the aerosol optical inlet sampled inside the forest canopy and alternated between PM_1 and PM_{10} size cuts. Particle light scattering was measured with a TSI 3563 integrating nephelometer at 450, 550, and 700 nm, while particle light absorption was measured with Magee Scientific AE31 and AE33 aethalometers at seven wavelengths and harmonized with co-located absorption measurements where required. Size-resolved PM mass was obtained from Dekati gravimetric cascade-impactor filter samples collected over 2–3 d intervals, providing mass fractions for PM_1, intermediate supermicron fractions, PM_{10}, and super-PM_{10} aerosol particles. Optical variables were averaged over the same impactor sampling intervals before merging with the PM-mass and event-classification data. Aerosol particle size distributions were derived from combined mobility and aerodynamic particle size-distribution measurements following long-term atmospheric aerosol measurement practice (Banerji et al., 2025; Luoma et al., 2019; Wiedensohler et al., 2012). Detailed information on the measurement site, instruments, derived variables, operational size ranges, and valid-count differences is provided in the Supporting Information, Sect. S3.

2.2 Operational event labels and background definition

Dust-affected sampling intervals were identified using the processed long-range-transported dust-event indicator based on the Finland dust-event inventory of Varga et al. (2023), which used MERRA-2 aerosol reanalysis dust column mass density fields followed by multistep verification with independent satellite, aerosol, trajectory, and synoptic evidence. Pollen-positive sampling intervals were identified from the cascade-impactor filter records following the approach of Banerji et al. (2025). When pollen material was observed on at least one corresponding cascade-impactor size-fraction filter, the complete 2–3 d impactor sampling interval was classified as pollen affected in the merged optical–PM-mass dataset. This definition includes pollen detected in any measured impactor size fraction; 6 of the 21 pollen-positive intervals were identified solely from pollen detected in the super-PM_{10} fraction. The resulting pollen indicator is therefore an interval-level flag derived from filter evidence, not a pollen concentration or a direct continuous particle-count measurement. The dust and pollen labels were therefore not derived from identical source-measurement methods: the dust label represents an externally identified transported-dust period based on a MERRA-2-supported and independently verified long-range transport inventory, whereas the pollen label

https://doi.org/10.5194/egusphere-2026-3400
Preprint. Discussion started: 1 July 2026

represents filter-based evidence for pollen material during the sampling interval. In addition, the pollen-positive flag and the PM-mass variables share the cascade-impactor sampling framework in the merged optical–PM-mass dataset, so PM-mass contrasts are not treated as independent validation of the pollen label. The comparisons below should accordingly be read as contrasts between two operational event classes rather than as a controlled source-apportionment experiment. Background denotes the non-event reference population at SMEAR II, not aerosol-free or source-free air. In the merged optical–PM-mass dataset, background sampling intervals were intervals classified as neither pollen positive nor dust affected after applying the operational event-label filters. Background observations can therefore still include ordinary boreal aerosol variability from NPF, biogenic emissions, meteorology, transport, and other unclassified sources. No dust–pollen overlap occurred in the merged optical–PM-mass dataset, so no class-priority rule affected the final labels. Further details of the classification logic and final exclusive counts are provided in the Supporting Information, Sect. S1 and Table S1.

2.3 Observation units and sample-size accounting

To distinguish the observational unit from a temporally distinct atmospheric occurrence, we use three terms. A *sampling interval* is one 2–3 d cascade-impactor collection period and one row of the merged optical–PM-mass dataset. An *event-affected observation* is a sampling interval or native-resolution APSD observation carrying a dust or pollen label. An *event episode* is a temporally distinct cluster obtained by declustering the native-resolution APSD observations. Accordingly, "dust-event observations" and "pollen-event observations" in sampling-interval-level or timestamp-level comparisons denote labelled observations and are not assumed to be independent events. We reserve "event-level" results for analyses based on the declustered episode medians. This distinction follows earlier SMEAR II particle-size-distribution studies, where aerosol records were interpreted using event and nonevent classifications rather than as independent high-frequency replicates (Dal Maso et al., 2005; Buenrostro Mazon et al., 2009; Dada et al., 2017). It also reflects the broader time-series issue that atmospheric measurements commonly exhibit serial dependence, so repeated measurements within one atmospheric episode can inflate the apparent sample size if treated as independent (Collaud Coen et al., 2020). Declustering reduces within-event temporal dependence but does not guarantee complete statistical independence among episodes.

The merged optical–PM-mass dataset contained 1581 sampling intervals before variable-specific missing-value filtering. The final classification identified 1545 background sampling intervals, 21 pollen-positive sampling intervals, and 15 dust-affected sampling intervals, corresponding to 36 event-affected sampling intervals (Table S1). These counts must not be interpreted as numbers of pollen- or dust-affected calendar days or as numbers of statistically independent atmospheric episodes. The operational-label audit is provided in Sect. S10 and Table S15, and the complete inventory of the 36 labelled merged optical–PM-mass sampling intervals is provided in Sect. S10 and Table S16. Dust-affected intervals occurred from February to August, whereas pollen-positive intervals occurred from April to June, with the largest number of pollen-positive intervals in May (Table S2). Variable-specific valid counts differed after filtering. For example, the main PM-mass variables had 1563 valid observations, while PM_1 $\sigma_{sca,550}$ and $PM_{1–10}$ $\sigma_{sca,550}$ had 1481 and 1474 valid observations, respectively (Table S4). The larger optical-only data availability was treated separately from the merged optical–PM-mass statistics; the optical-only counts

https://doi.org/10.5194/egusphere-2026-3400
Preprint. Discussion started: 1 July 2026

are reported only as instrumental availability diagnostics and are not used as the sample sizes for the merged optical–PM-mass comparisons (Sect. S2 and Table S3).

2.4 Statistical analysis

2.4.1 Purpose and labelled contrasts

All statistical comparisons were conducted after variable-specific missing-value filtering. Because many aerosol variables were right-skewed and contained occasional large values, continuous variables were summarized using medians and interquartile ranges (IQRs), and the main contrasts were expressed as differences between group medians. The statistical framework is therefore a retrospective effect-size and uncertainty analysis. Its purpose is to describe which measured or derived variables change during labelled dust- and pollen-affected periods, and which variables retain a dust–pollen contrast after temporal-control and event-level sensitivity checks. It is not intended to train, validate, or propose a predictive event-classification algorithm. The analysis separated event detection from event typing. Event detection compared the pooled event-affected class, $E = D \cup P$, with background, B, where D denotes dust-affected observations and P denotes pollen-positive observations. Dust–pollen typing compared D with P within the event-affected subset. In the merged optical–PM-mass analysis, these symbols represent classified sampling intervals; in the event-level APSD analysis, they represent declustered episode medians. For a measured or derived variable X, event detection was quantified as a background-IQR-scaled median shift,

$$\Delta^{*}_{\mathrm{det}}(X) = \frac{\mathrm{median}(X|E) - \mathrm{median}(X|B)}{\mathrm{IQR}(X|B)}. \tag{1}$$

Dust–pollen typing was quantified as

$$\Delta^{*}_{\mathrm{typ}}(X) = \frac{\mathrm{median}(X|D) - \mathrm{median}(X|P)}{\mathrm{IQR}(X|B)}. \tag{2}$$

The direction of $\Delta^{*}_{\mathrm{typ}}$ is therefore dust minus pollen. Positive values indicate larger values in the dust-affected group, while negative values indicate larger values in the pollen-affected group. Unstandardized median differences were retained in the original measurement units, while the IQR-scaled values were used to compare effect magnitudes across variables with different units and ranges.

This normalization is central to the interpretation because it prevents the analysis from ranking variables simply because they are expressed in large numerical units. A variable is considered useful only when its effect direction, standardized magnitude, uncertainty, temporal robustness, and physical meaning are mutually consistent. The framework therefore functions as an evidence audit for labelled atmospheric episodes: it identifies variables that respond to event occurrence, tests whether those variables also retain dust–pollen information, and makes clear when the evidence is too dependent on sampling interval, season, diurnal timing, or a small number of episodes.

2.4.2 Merged optical–PM-mass uncertainty

For the merged optical–PM-mass analysis, the classified sampling interval was the observational unit entering the group comparisons. Uncertainty in the median differences was quantified using 95 % percentile confidence intervals from 5000 block-

https://doi.org/10.5194/egusphere-2026-3400
Preprint. Discussion started: 1 July 2026

bootstrap resamples (Efron and Tibshirani, 1994; Künsch, 1989). Contiguous day blocks were resampled with replacement to preserve temporal dependence within sampling periods, a concern widely recognized for atmospheric measurement time series (Collaud Coen et al., 2020). A data-driven procedure selected the block length separately for each particle-size fraction and feature set using the sampling-interval duration and the decay of the background autocorrelation function, with the selected length constrained to 1–3 d. This day-blocking is pseudo-daily only in the resampling sense: the measurements themselves remain the 2–3 d cascade-impactor sampling intervals used in the supermicron aerosol framework of Banerji et al. (2025), while calendar-day blocks are used to keep adjacent intervals together during bootstrap resampling. Cliff's δ and two-sided Mann–Whitney tests were calculated as supporting non-parametric distributional measures (Cliff, 1993; Mann and Whitney, 1947; Vargha and Delaney, 2000). Cliff's δ describes the direction and degree of pairwise dominance between two groups: positive values indicate that the first group tends to have larger values, negative values indicate the opposite, and values near zero indicate substantial distributional overlap. Because several related optical, PM-mass, and APSD-derived variables were examined, individual p values were not used as stand-alone discovery criteria. Instead, conclusions were based primarily on effect direction, magnitude, confidence-interval width, consistency across related variables and sensitivity analyses, and physical interpretability; Mann–Whitney p values were treated as supporting diagnostics.

2.4.3 APSD metrics and temporal background correction

Particle number size distributions were constructed from differential mobility particle sizer (DMPS) and aerodynamic particle sizer (APS) measurements after applying instrument-specific size limits. The DMPS-based mobility size-distribution measurements follow the long-term atmospheric particle number size-distribution measurement framework used at SMEAR-type stations and related European aerosol networks (Wiedensohler et al., 2012). The distributions were expressed as number, cross-sectional-area, and volume distributions. Cross-sectional-area and volume distributions were used to connect particle-size structure to scattering-relevant particle area and particulate material (Seinfeld and Pandis, 2016). The main APSD-derived metrics were accumulation-mode cross-sectional area, S_{acc}; accumulation-mode volume, V_{acc}; coarse-mode volume, V_{coarse}; the volume-ratio metric, R_V; and Aitken-mode number concentration, N_{Ait}. Because the DMPS and APS characterize particle size using different equivalent diameters, APSD-derived cross-sectional-area and volume metrics should be interpreted as operational size-distribution metrics unless aerodynamic diameters are converted to geometric or volume-equivalent diameters using explicit density and shape assumptions (Sect. S3).

The APSD-derived metrics were analysed separately at their native time resolution and therefore had much larger timestamp-level sample sizes than the merged optical–PM-mass dataset (Sect. S7 and Table S9). To reduce confounding by seasonal and diurnal changes in the boreal background aerosol, two anomaly forms were examined. Month anomalies were obtained by subtracting the corresponding background calendar-month median from each observation. Month-plus-hour anomalies were obtained by subtracting the background median for the corresponding calendar month and hour of day and were used as the preferred temporal correction. The preferred Pool B background baseline was restricted to 2011–2014 because all pollen-positive observations occurred within this period; restricting the background to the same pollen-observation era reduced confounding from longer-term differences in data coverage. A stricter common-support-year baseline was used as a sensitivity

https://doi.org/10.5194/egusphere-2026-3400
Preprint. Discussion started: 1 July 2026

check. These anomaly comparisons test whether dust–pollen differences persist after removal of typical seasonal and diurnal background structure. They reduce, but cannot eliminate, confounding by meteorology, transport history, source timing, and local phenological conditions; consequently, the controlled APSD contrasts are interpreted as receptor-site associations rather than source-intrinsic properties.

APSD records from the same event-affected period are repeated measurements. They are time-correlated, so they are not independent event replicates. We used two sensitivity checks for temporal dependence.

2.4.4 Event declustering and temporal-dependence sensitivity

First, month-plus-hour anomalies were declustered within each event class into event episodes. Operationally, a new episode was defined when the gap between consecutive observations was at least 48 h. The 48 h threshold is an operational run-declustering choice, not a physical lifetime for dust or pollen events. Similar event-sequence or run-declustering logic is used in atmospheric extreme-event and dust-event analyses to avoid treating closely spaced, temporally correlated records as fully independent events (Tuel and Martius, 2021; Sarafian et al., 2023). Each episode was then represented by one median anomaly, yielding 15 dust episodes and 8 pollen episodes that were treated as the event-level units of inference. These episode counts were derived from the native-resolution APSD records and must not be equated with the 15 dust-affected and 21 pollen-positive sampling intervals in the merged optical–PM-mass dataset. As a threshold sensitivity check, the declustering was repeated with 24, 48, and 72 h gap criteria. The 24 h threshold yielded 15 dust and 9 pollen episodes, whereas the 48 and 72 h thresholds produced the same episode lists, with 15 dust and 8 pollen episodes. Thus, the 24 h threshold split one additional pollen episode, but the dust-minus-pollen median-difference directions were unchanged for all five APSD metrics (Table S12). The complete declustered APSD episode inventory and episode-median anomaly values are provided in Sect. S10 and Tables S17–S18. The 48 h rule reduces dependence among the event-level units but cannot establish that all episodes are fully independent. Event-level dust–pollen differences were evaluated using median differences, Cliff's δ, Mann–Whitney tests, and 95 % confidence intervals from 2000 balanced bootstrap resamples of the episode medians.

Second, as a sensitivity check that retained the timestamp-level data, 24 h moving-block bootstraps with 2000 resamples were used to preserve short-term dependence within the anomaly series (Künsch, 1989).

2.4.5 Evidence hierarchy

The APSD results were interpreted using an explicit hierarchy of evidence. Native-resolution contrasts quantified the observed distributional differences and their persistence after month and month-plus-hour correction, but were treated primarily as descriptive because many timestamps originated from the same event-affected periods. Greater inferential weight was placed on consistency of effect direction across temporal corrections, declustered episode-level comparisons, declustering-threshold sensitivity, moving-block-bootstrap sensitivity analyses, and leave-one-episode-out checks, in which the dust–pollen contrast is recalculated after removing one dust or pollen episode at a time. Very small timestamp-level p values were not treated as primary evidence. A confidence interval crossing zero indicates that the data are compatible with no difference and with effects in either direction; it does not establish the absence of a physically meaningful difference. Because only 15 dust and 8 pollen

https://doi.org/10.5194/egusphere-2026-3400
Preprint. Discussion started: 1 July 2026

episodes remained after the primary 48 h declustering, wide event-level intervals were interpreted as evidence of substantial uncertainty and limited precision. Accordingly, the results are presented as physically interpretable event-type tendencies and not as a definitive operational classification model. Further statistical definitions, unit-of-inference considerations, and sensitivity results are provided in Sect. S4 and Tables S10–S14.

The complete analysis workflow is summarized in Figure 1. The schematic emphasizes that the methodology is a retrospective non-parametric effect-size framework for interpreting labelled observations, not a prediction mechanism or a real-time classifier.

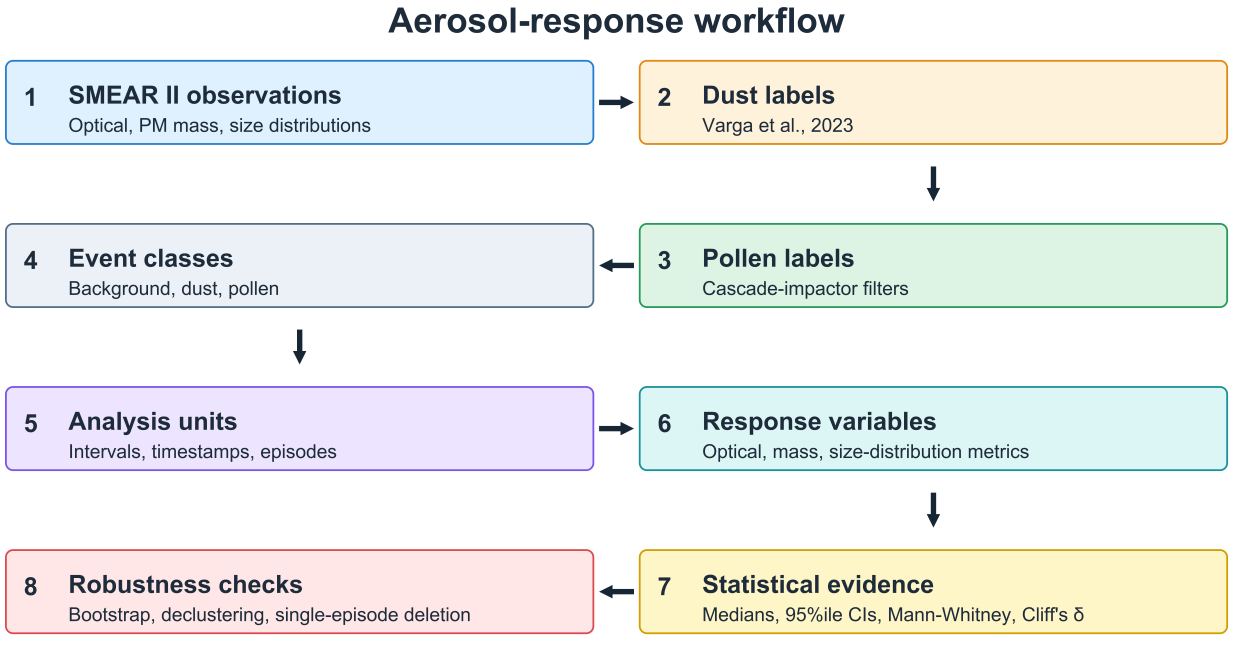

Figure 1. Aerosol-response workflow. SMEAR II optical, PM-mass, and aerosol particle size-distribution observations were combined with two event-evidence streams: transported-dust labels from the MERRA-2-supported inventory and verification procedure of Varga et al. (2023), and pollen-positive labels from the Hyytiälä cascade-impactor filter evidence described by Banerji et al. (2025). The workflow assigns background, dust, and pollen classes; separates sampling intervals, native timestamps, and declustered episodes; derives response variables; evaluates median contrasts with non-parametric uncertainty and dominance diagnostics; and applies bootstrap, declustering, and single-episode deletion checks. It is a retrospective receptor-site workflow, not a predictive source classifier.

https://doi.org/10.5194/egusphere-2026-3400
Preprint. Discussion started: 1 July 2026

3 Results and Discussion

3.1 Optical-property response during dust- and pollen-affected periods

Dust- and pollen-affected sampling intervals both showed enhanced aerosol light scattering relative to background sampling intervals in the merged optical–PM-mass analysis (Figure 2). For PM_1 $\sigma_{sca,550}$, the standardized event–background median shift was $\Delta^*_{det} = 0.88$, with a raw median-difference confidence interval of 3.85–12.29 Mm^{-1} and Cliff's $\delta = 0.463$. $PM_{1–10}$ $\sigma_{sca,550}$ also increased under event-affected conditions, although more weakly, with $\Delta^*_{det} = 0.81$, a confidence interval of 0.48–2.88 Mm^{-1}, and Cliff's $\delta = 0.342$. These sampling-interval-level effect sizes refer to the merged optical–PM-mass dataset, where the corresponding valid observation counts were 1481 and 1474, respectively (Table S4). The full event-detection effect-size results are provided in Table S5.

The optical event-detection response did not translate into robust dust–pollen typing. The dust–pollen median-difference confidence intervals crossed zero for both PM_1 and $PM_{1–10}$ $\sigma_{sca,550}$ (Table S6). SAE also provided limited source-type information. PM_1 SAE showed a small event–background response, with $\Delta^*_{det} = 0.38$ and a confidence interval of 0.08–0.21, while $PM_{1–10}$ SAE did not show a robust event-detection response (Table S5). Dust–pollen SAE typing was not robust in either size fraction (Table S6).

This behaviour is consistent with the non-unique nature of aerosol optical signatures. Scattering and SAE respond to particle number, particle size, hygroscopicity, refractive index, and mixing state, so physically different aerosol perturbations can produce overlapping optical responses (Schuster et al., 2006; Seinfeld and Pandis, 2016; Titos et al., 2021). Thus, the optical variables answered whether an aerosol perturbation occurred, but not reliably which event type occurred.

3.2 Size dependence of PM-mass responses

Size-resolved PM mass showed a stronger size dependence than the optical variables (Figure 3). Event detection increased from PM_1 mass to $PM_{1–10}$ mass and super-PM_{10} mass, defined operationally here as the derived mass fraction above 10 μm. PM_1 mass had $\Delta^*_{det} = 1.01$ and a median-difference confidence interval of 1.55–3.88 $\mu g\ m^{-3}$. $PM_{1–10}$ mass had $\Delta^*_{det} = 1.64$ and a confidence interval of 1.28–7.07 $\mu g\ m^{-3}$. The strongest event-detection response occurred for super-PM_{10} mass, with $\Delta^*_{det} = 3.72$ and a confidence interval of 1.56–5.68 $\mu g\ m^{-3}$ (Table S5). These PM-mass statistics were calculated from the merged optical–PM-mass dataset, in which each of the main PM-mass variables had 1563 valid observations (Table S4).

Dust–pollen typing showed a different pattern from event detection. PM_1 mass and PM_{10} mass did not robustly distinguish dust from pollen because their dust–pollen confidence intervals crossed zero (Table S6). The clearest mass-based labelled-class contrast occurred for $PM_{1–10}$ mass, where the dust–pollen contrast was negative: $\Delta^*_{typ} = -3.25$, with a median difference of $-4.83\ \mu g\ m^{-3}$ and a confidence interval of -7.26 to $-0.53\ \mu g\ m^{-3}$ (Table S6). Because the contrast is defined as dust minus pollen, this indicates higher $PM_{1–10}$ mass during pollen-positive sampling intervals than during dust-affected sampling intervals in the present event set. super-PM_{10} mass showed a similar negative tendency, but its bootstrap confidence interval slightly crossed zero, so it is interpreted as a distributional tendency rather than as a clean median-shift result. The mass-based

https://doi.org/10.5194/egusphere-2026-3400
Preprint. Discussion started: 1 July 2026

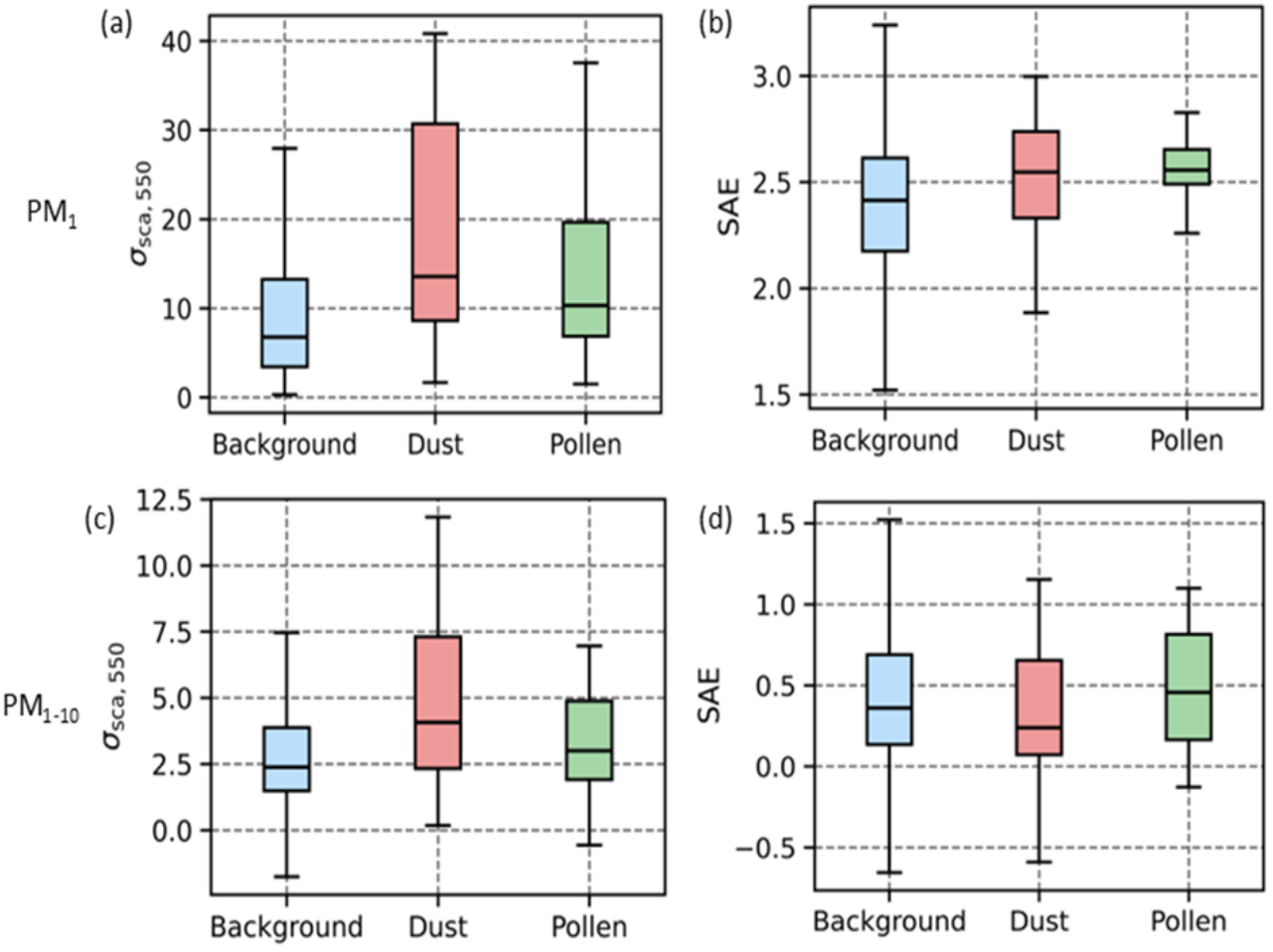

Figure 2. Aerosol optical-property response during background, dust-affected, and pollen-positive sampling intervals in the merged optical–PM-mass analysis. Panels show PM_1 scattering, PM_1 SAE, $PM_{1–10}$ scattering, and $PM_{1–10}$ SAE. Boxes show the interquartile range, horizontal lines indicate medians, and whiskers show the 5th–95th percentile range. Both dust- and pollen-affected intervals show enhanced scattering relative to background intervals, but their optical distributions overlap substantially.

https://doi.org/10.5194/egusphere-2026-3400
Preprint. Discussion started: 1 July 2026

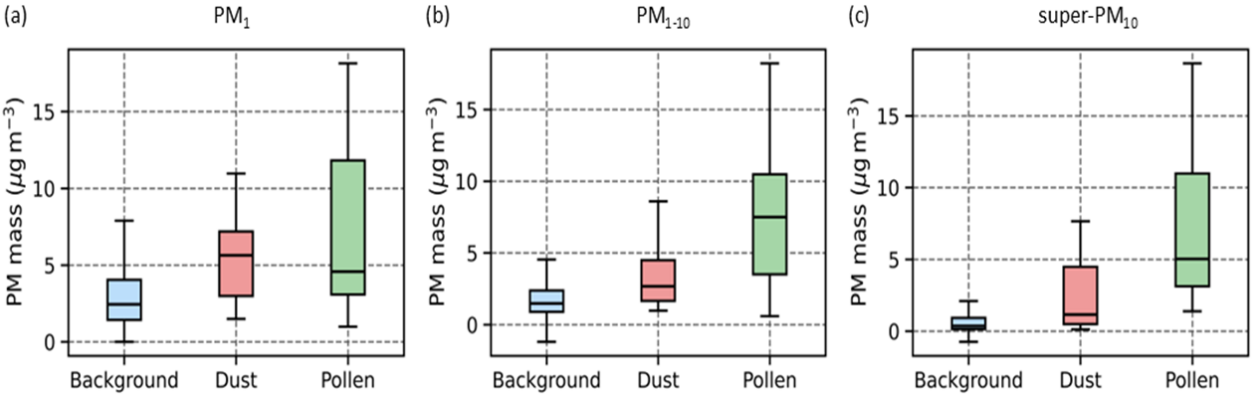

Figure 3. Size-resolved PM-mass response during background, dust-affected, and pollen-positive sampling intervals in the merged optical–PM-mass analysis. Panels show PM_1 mass, $PM_{1–10}$ mass, and super-PM_{10} mass. Boxes show the interquartile range, horizontal lines indicate medians, and whiskers show the 5th–95th percentile range. Event-related PM-mass enhancement strengthens with particle size. Because the pollen-positive label and PM-mass variables both derive from the cascade-impactor sampling framework, these panels are interpreted as PM-mass response diagnostics rather than independent source-validation tests.

typing results are therefore useful for describing the labelled event set, but they are not interpreted as an independent classifier of dust and pollen source type.

This size dependence is physically consistent with the approximate cubic scaling of particle volume, and therefore mass for particles of comparable density and morphology, with particle diameter (Seinfeld and Pandis, 2016). Coarse and supermicron particle changes can therefore produce large PM responses even when optical variables remain only weakly discriminatory. Negative derived mass values occurred only under background conditions and did not drive the PM-mass conclusions (Sect. S6 and Table S7). Excluding negative derived mass values produced only minor changes in the effect-size estimates, including a change in super-PM_{10} detection Δ^* from 3.72 to 3.58 and a change in $PM_{1–10}$ typing Δ^* from -3.25 to -3.24 (Table S8).

3.3 APSD-derived area and volume responses

The weak source specificity of the optical variables and the stronger size dependence of the PM-mass response indicate that event-type tendencies are more likely to be expressed in the redistribution of particles across size than in bulk optical enhancement alone. We therefore examined APSD-derived number, cross-sectional-area, and volume metrics. Both event classes modified the aerosol population, but the most persistent dust–pollen tendency occurred in accumulation-mode metrics rather than in bulk optical intensity or coarse-mode volume alone.

Under the Pool B month-plus-hour anomaly baseline (Figure 4), dust-affected observations had higher S_{acc} anomalies than pollen-positive observations, with $\Delta^* = 0.558$ and a median anomaly difference of 25.39 μm^2 cm^{-3}. The corresponding confidence interval, 17.10–31.98 μm^2 cm^{-3}, did not cross zero, indicating that the controlled S_{acc} contrast persisted after accounting for month and hour background structure at native time resolution (Table S10). After event declustering, the contrast retained the same positive direction and had a larger standardized effect, but the bootstrap confidence interval crossed zero and

https://doi.org/10.5194/egusphere-2026-3400
Preprint. Discussion started: 1 July 2026

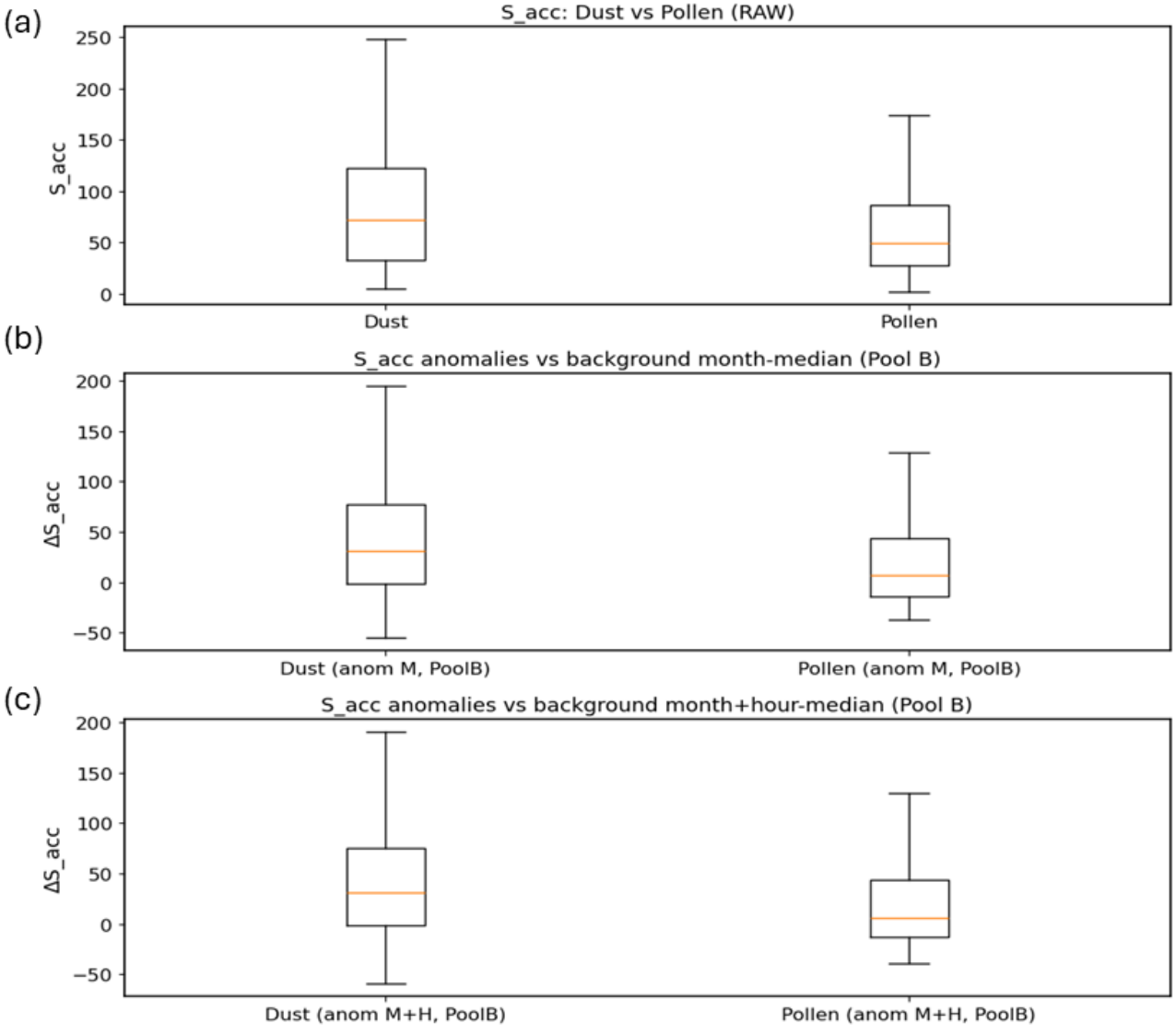

Figure 4. Confounding-controlled dust–pollen comparison for accumulation-mode cross-sectional area. Panel (a) shows the raw dust–pollen comparison. Panel (b) shows anomalies after subtracting the background month median, and panel (c) shows anomalies after subtracting the background month-plus-hour median. The persistence of the native-resolution dust–pollen difference after month-plus-hour correction suggests that the contrast is not explained solely by seasonal or diurnal background variability, but event-level uncertainty remains substantial because only 15 dust and 8 pollen episodes were available after declustering.

https://doi.org/10.5194/egusphere-2026-3400
Preprint. Discussion started: 1 July 2026

was therefore compatible with no episode-level difference and with effects in either direction (Table S11). The dust-minus-pollen direction of S_{acc} was unchanged when the declustering gap criterion was varied between 24, 48, and 72 h; the 48 and 72 h thresholds produced identical episode-level S_{acc} values, while the 24 h threshold retained the same positive direction despite one additional pollen episode (Table S12). Therefore, S_{acc} is interpreted as the clearest APSD-based tendency in this dataset, rather than as a stand-alone source-identification criterion.

Accumulation-mode volume, V_{acc}, showed a consistent supporting response, with $\Delta^* = 0.520$, a median anomaly difference of 1.00 μm^3 cm^{-3}, and a confidence interval of 0.686–1.238 μm^3 cm^{-3} in the native-resolution Pool B month-plus-hour anomaly analysis (Table S10). However, after event declustering, the V_{acc} dust–pollen confidence interval crossed zero (Table S11). Thus, V_{acc} supports the accumulation-mode interpretation but is treated as secondary evidence.

By contrast, coarse-mode volume, V_{coarse}, did not provide a robust dust–pollen separation. Its Pool B month-plus-hour anomaly confidence interval crossed zero, and the standardized effect was small at native time resolution (Table S10). The event-declustered analysis and moving-block-bootstrap sensitivity check also gave confidence intervals crossing zero (Table S11). The volume-ratio metric, R_V, was statistically separated in the native-resolution analysis but had a small standardized effect, and the event-declustered and moving-block-bootstrap sensitivity checks crossed zero (Tables S10 and S11). It is therefore best interpreted as secondary supporting information rather than as a primary event-type metric.

A leave-one-episode-out sensitivity analysis of the declustered episode medians showed no sign reversals for S_{acc}, V_{acc}, V_{coarse}, R_V, or N_{Ait} when any single dust or pollen episode was removed (Table S13). For each APSD-derived metric, the contrast was recalculated after deleting each of the 15 dust episodes and each of the 8 pollen episodes, giving 23 deletion tests per metric and 115 recalculated contrasts across the five metrics. Thus, the directions of the episode-median contrasts were not controlled by one individual episode. The largest absolute shifts were tied across multiple deletions, so the leave-one-episode-out analysis is interpreted as a sign-stability diagnostic rather than as evidence for a unique influential episode. The wide bootstrap intervals still indicate limited episode-level precision.

The apparently different directions of the $\mathrm{PM}_{1\text{–}10}$ mass and S_{acc} results are not contradictory because the two variables weight the size distribution differently. PM mass is approximately volume-weighted and scales with particle diameter cubed, so $\mathrm{PM}_{1\text{–}10}$ mass can be strongly influenced by larger supermicron and coarse-tail particles. In contrast, S_{acc} is an accumulation-mode cross-sectional-area metric that scales with particle diameter squared and is more directly linked to scattering-relevant particle geometry. Thus, pollen-positive intervals can show higher $\mathrm{PM}_{1\text{–}10}$ mass in the present event set, while dust-affected APSD observations can show higher controlled accumulation-mode cross-sectional area. This interpretation is a size-weighting and receptor-site consistency argument, not a direct chemical or morphological closure between the PM-mass and APSD measurements. The reconciliation is summarized in Sect. S8. The clearest source-type tendency was therefore not in bulk optical intensity alone, but in how aerosol area and mass were redistributed across particle size.

Additional diagnostic visualizations of the feature-screening logic, detection-versus-typing distinction, and volume-metric sensitivity are provided in Figures S7–S9. These figures are used only to summarize the screening framework; the interpretation above is based on the effect-size tables, confidence intervals, event-declustered analyses, moving-block-bootstrap checks, and leave-one-episode-out diagnostics.

https://doi.org/10.5194/egusphere-2026-3400
Preprint. Discussion started: 1 July 2026

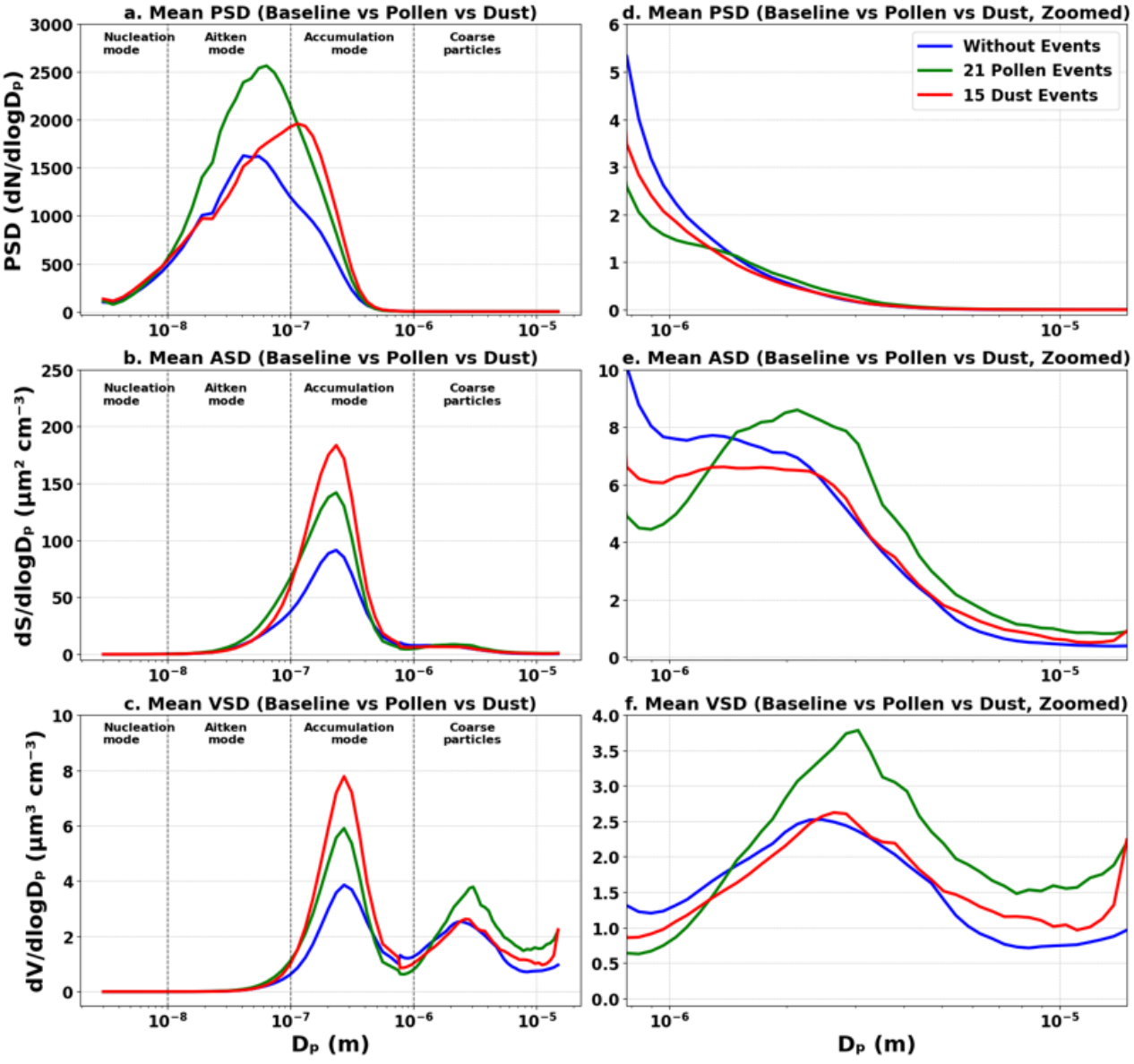

Figure 5. Mean aerosol particle size distributions during background, pollen-positive, and dust-affected conditions. Panels (a)–(c) show the full-range mean particle number size distribution (PSD), cross-sectional-area size distribution (SAD), and volume size distribution (VSD), respectively. Panels (d)–(f) show the corresponding zoomed larger-particle ranges for PSD, SAD, and VSD. Blue, green, and red lines denote non-event background, pollen-positive, and dust-affected conditions, respectively. The comparison illustrates that the two operational event classes can produce non-unique bulk optical responses while redistributing particle number, cross-sectional area, and volume differently across particle diameter.

https://doi.org/10.5194/egusphere-2026-3400
Preprint. Discussion started: 1 July 2026

The mean size distributions further illustrate why the optical and PM-mass responses are not equivalent (Figure 5). In the particle number size distribution, event-period differences extend into the Aitken-mode size range, especially during pollen-positive periods. In the cross-sectional-area and volume size distributions, however, the more relevant dust–pollen differences shift toward the accumulation and larger-particle size ranges. This supports the interpretation that $PM_{1–10}$ mass and S_{acc} need not show the same dust–pollen direction because they weight the particle size distribution differently.

3.4 Sub-100 nm particle behaviour as process context

The motivation for examining the sub-100 nm size range came from the mean particle number size distributions, where event-period differences extended into the Aitken-mode size range. Because intact dust and pollen particles are not primarily sub-100 nm particles, this feature should not be interpreted directly as a source signature. At SMEAR II, nucleation- and Aitken-mode variability is strongly influenced by new-particle formation and early growth processes (Dal Maso et al., 2005; Dada et al., 2017). Dust can also interact with NPF through competing mechanisms, including condensation-sink effects and dust-related photochemistry, but these effects are site and condition dependent (Nie et al., 2014; Casquero-Vera et al., 2023). Similarly, pollen may contribute to submicron particles through rupture, fragmentation, or release of subpollen particles, but this is distinct from classical gas-to-particle NPF (Steiner et al., 2015; Hendrickson et al., 2023).

The 100 nm cutoff was used as a practical diagnostic boundary rather than as a strict physical threshold. Particles below 100 nm largely represent the nucleation- and Aitken-mode size range, where NPF, early growth, and survival against losses to the pre-existing aerosol population are most relevant. In contrast, particles above about 100 nm increasingly contribute to accumulation-mode cross-sectional area, volume, PM mass, light scattering, and potential cloud-condensation-nuclei relevance. However, the transition is not fixed, because CCN activation depends on particle size, hygroscopicity, composition, mixing state, and supersaturation. Example NPF-like and non-NPF-like cases during both dust and pollen event periods are shown in Figure 6. These examples illustrate that sub-100 nm particle evolution is not uniquely determined by the dust or pollen event label.

We therefore treat the sub-100 nm analysis as process-level context rather than as a primary dust–pollen typing criterion. Although raw Aitken-mode number concentration was higher during pollen-positive observations than during dust-affected observations, this contrast weakened after temporal correction and event declustering (Table S14). Thus, the main dust–pollen interpretation is based on size-resolved PM mass and APSD-derived accumulation/coarse particle metrics, not on sub-100 nm variability alone.

The full interval-resolved sub-100 nm particle number, volume, and cross-sectional-area size-distribution panels for all pollen-positive and dust-affected sampling intervals are provided in Figures S1–S6. These Supporting Information figures document the variability among labelled intervals and support the interpretation that sub-100 nm structure is process context rather than a dust- or pollen-specific source marker.

https://doi.org/10.5194/egusphere-2026-3400
Preprint. Discussion started: 1 July 2026

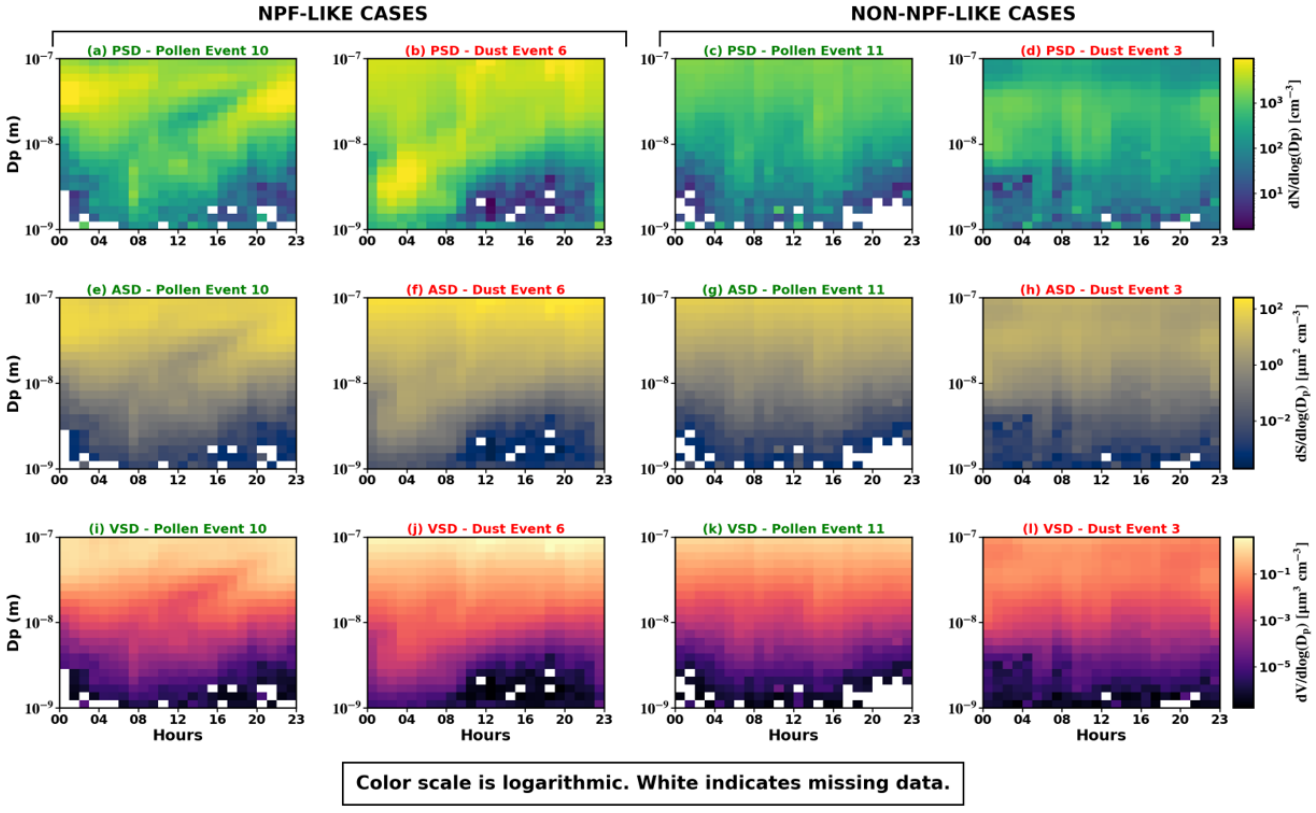

Figure 6. Example sub-100 nm particle size-distribution behaviour during selected pollen-positive and dust-affected periods with and without NPF-like behaviour. Columns show representative NPF-like and non-NPF-like cases for pollen-positive and dust-affected periods. Rows show particle number size distributions, cross-sectional-area size distributions, and volume size distributions below 100 nm. The selected examples are illustrative and are not used for statistical inference.

3.5 Implications

These results have three implications for interpreting this boreal aerosol event record and similar receptor-site analyses. First, bulk optical enhancement is not sufficient evidence for event type. Dust-affected and pollen-positive periods both enhanced aerosol scattering, and their optical signatures overlapped. Source typing based only on $\sigma_{\mathrm{sca},550}$ or SAE could therefore be misleading.

Second, size-resolved information is essential for this event set. Event occurrence was most strongly detected in larger PM fractions, especially super-PM_{10} mass, while event type was better expressed in $PM_{1–10}$ mass and accumulation-mode APSD metrics. Among the APSD metrics, the clearest and most persistent dust–pollen tendency was found in S_{acc}, supported by V_{acc}, rather than in coarse-mode volume. This indicates that the operationally classified dust- and pollen-affected periods influenced the receptor-site aerosol population through different redistributions of accumulation-mode area and volume, even when their bulk optical responses overlapped.

https://doi.org/10.5194/egusphere-2026-3400
Preprint. Discussion started: 1 July 2026

Third, sub-100 nm particle behaviour should be interpreted as process context rather than as a primary event-typing signal. Event-period sub-100 nm structure can reveal whether nucleation- and Aitken-mode processes were active, but the strongest dust–pollen information in this analysis was found in size-resolved PM mass and APSD-derived accumulation/coarse particle metrics.

Fourth, the framework has broader methodological implications for atmospheric event studies. Long-term observatory datasets commonly combine operational labels, uneven event counts, non-normal aerosol variables, and serially dependent observations. In such cases, a retrospective effect-size framework provides a reproducible intermediate step between qualitative event description and predictive source classification. It can be used to screen which variables carry physically meaningful event information before investing in site-transfer tests, chemical or microphysical source validation, or supervised classification. Applied across additional years, sites, and event types, the same framework could help determine whether a candidate dust, pollen, smoke, sea-salt, or biological-aerosol indicator is site-specific or transferable across receptor environments.

The main limitations follow directly from the observational design. The event labels are operational and were derived from different evidence streams for dust and pollen; therefore, the study tests labelled receptor-site event classes rather than controlled source samples. The pollen-positive label and PM-mass variables also share the cascade-impactor sampling framework, so PM-mass contrasts describe responses within the labelled event set and should not be treated as independent validation of pollen source type. The number of independent APSD episodes is small, especially for pollen, which limits precision even when effect directions are stable under threshold and leave-one-episode-out sensitivity checks. Finally, SMEAR II is a well-characterized boreal forest receptor site, but dust and pollen sources, transport pathways, meteorology, and phenology are site dependent. The results are therefore most appropriately used as a mechanistic case study of event detection and event typing at SMEAR II, not as a universal boreal classification rule.

4 Conclusions

Dust- and pollen-affected periods both perturbed the aerosol population at SMEAR II, but the response was not expressed equally across optical, PM-mass, and size-distribution variables. Both event classes enhanced aerosol scattering relative to the non-event background. However, scattering coefficients and scattering Ångström exponents overlapped strongly between dust-affected and pollen-positive observations and did not provide robust event typing.

Event detection was strongest in variables that captured enhanced particle loading, especially larger PM fractions. The clearest event–background response occurred for super-PM_{10} mass, showing that event occurrence at the receptor site was most strongly expressed through size-resolved mass enhancement. Because the pollen-positive label and PM-mass variables share the cascade-impactor sampling framework, these PM-mass results are interpreted as responses within the labelled event set rather than as independent validation of pollen source type.

The variables that detected event occurrence were not always the variables that distinguished dust from pollen. $PM_{1–10}$ mass gave the clearest mass-based dust–pollen contrast in the present event set. Among APSD-derived metrics, accumulation-mode cross-sectional area, S_{acc}, showed the clearest temporally controlled dust–pollen tendency, with support from accumulation-

https://doi.org/10.5194/egusphere-2026-3400
Preprint. Discussion started: 1 July 2026

mode volume, V_{acc}. Coarse-mode volume did not robustly distinguish event type. Thus, dust–pollen differences were expressed more clearly in the size-resolved redistribution of aerosol area and mass than in bulk optical enhancement alone.

Sub-100 nm particle behaviour provided process context, not a primary event-typing criterion. Differences in the Aitken-mode size range motivated the sub-100 nm analysis, but these differences weakened after temporal correction and event declustering. The sub-100 nm results therefore describe concurrent aerosol processes during event periods rather than direct dust or pollen source signatures.

The main limitations are the operational nature of the labels, the different evidence streams for dust and pollen, the shared cascade-impactor basis of pollen flags and PM mass, and the small number of declustered episodes, especially for pollen. The results should therefore be interpreted as physically interpretable receptor-site tendencies, not as a universal boreal dust–pollen classifier. The broader methodological message is that in-situ aerosol event studies should separate variables that detect an aerosol perturbation from variables that help interpret the type of perturbation. Future work can test the transferability of these tendencies by applying the same event-detection and event-typing framework at additional sites and by adding independent chemical, lidar, microscopic, or biological source constraints.

Code and data availability.

SMEAR II observational data are subject to the station data policy and data-access procedures. The analysis codes are available in the Zenodo repository (https://doi.org/10.5281/zenodo.20617239), and the processed data, including the analysis-ready tables, event-label inventories, and declustering-sensitivity outputs supporting the results, are available in a separate Zenodo repository (https://doi.org/10.5281/zenodo.20617554).

Supplement.

The supplement related to this article is provided as a separate PDF file. It contains the event-label and event-count audit, observation-count tables, instrument and derived-variable descriptions, statistical definitions, complete effect-size and sensitivity tables, diagnostic figures, interval-resolved sub-100 nm particle-size-distribution panels, and the complete event inventories.

Author contributions.

S.B., V.-M.K., and T.P. conceptualized the study. S.B. and T.G. performed the data analysis. S.B. wrote the original draft and prepared the manuscript with input from V.-M.K. and T.P. V.-M.K. and T.P. contributed to the review and revision of the manuscript, including the final edits. V.-M.K. and T.P. provided overall supervision. T.P. secured the funding to conduct the study.

Competing interests.

At least one of the (co-)authors is a member of the editorial board of Atmospheric Chemistry and Physics. The peer-review process will be guided by an independent editor, and the authors also have no other competing interests to declare.

https://doi.org/10.5194/egusphere-2026-3400
Preprint. Discussion started: 1 July 2026

Disclaimer.

Publisher's note: Copernicus Publications remains neutral with regard to jurisdictional claims made in the text, published maps, institutional affiliations, or any other geographical representation in this paper. While Copernicus Publications makes every effort to include appropriate place names, the final responsibility lies with the authors.

Acknowledgements.

The authors thank the technical staff of SMEAR II for their support. During the preparation of this manuscript, the authors used ChatGPT for language editing and to improve the readability and clarity of selected sections. After using this tool, the authors reviewed and edited the content as needed and take full responsibility for the content of the manuscript.

Financial support.

This work was supported by the Research Council of Finland via ACTRIS-FI (grant no. 328616), INAR RI (grant no. 345510), INAR RI Urban (grant no. 358647), INAR RI Integra (grant no. 367739), the ACCC Flagship (grant nos. 337549, 357902, 359340, and 374287), and the European Commission via the FOCI project (project no. 101056783).

https://doi.org/10.5194/egusphere-2026-3400
Preprint. Discussion started: 1 July 2026

References

Banerji, S., Luoma, K., Ylivinkka, I., Ahonen, L., Kerminen, V.-M., and Petäjä, T.: Measurement report: Optical properties of supermicron aerosol particles in a boreal environment, Atmospheric Chemistry and Physics, 25, 16 895–16 914, https://doi.org/10.5194/acp-25-16895-2025, 2025.

Bohlmann, S., Shang, X., Giannakaki, E., Filioglou, M., Saarto, A., Romakkaniemi, S., and Komppula, M.: Detection and characterization of birch pollen in the atmosphere using a multiwavelength Raman polarization lidar and Hirst-type pollen sampler in Finland, Atmospheric Chemistry and Physics, 19, 14 559–14 569, https://doi.org/10.5194/acp-19-14559-2019, 2019.

Bohlmann, S., Shang, X., Vakkari, V., Giannakaki, E., Leskinen, A., Lehtinen, K. E. J., Pätsi, S., and Komppula, M.: Lidar depolarization ratio of atmospheric pollen at multiple wavelengths, Atmospheric Chemistry and Physics, 21, 7083–7097, https://doi.org/10.5194/acp-21-7083-2021, 2021.

Buenrostro Mazon, S., Riipinen, I., Schultz, D. M., Valtanen, M., Dal Maso, M., Sogacheva, L., Junninen, H., Nieminen, T., Kerminen, V.-M., and Kulmala, M.: Classifying previously undefined days from eleven years of aerosol-particle-size distribution data from the SMEAR II station, Hyytiälä, Finland, Atmospheric Chemistry and Physics, 9, 667–676, https://doi.org/10.5194/acp-9-667-2009, 2009.

Casquero-Vera, J. A., Pérez-Ramírez, D., Lyamani, H., Rejano, F., Casans, A., Titos, G., Olmo, F. J., Dada, L., Hakala, S., Hussein, T., Lehtipalo, K., Paasonen, P., Hyvärinen, A., Pérez, N., Querol, X., Rodríguez, S., Kalivitis, N., González, Y., Alghamdi, M. A., Kerminen, V.-M., Alastuey, A., Petäjä, T., and Alados-Arboledas, L.: Impact of desert dust on new particle formation events and the cloud condensation nuclei budget in dust-influenced areas, Atmospheric Chemistry and Physics, 23, 15 795–15 814, https://doi.org/10.5194/acp-23-15795-2023, 2023.

Cliff, N.: Dominance statistics: Ordinal analyses to answer ordinal questions., Psychological Bulletin, 114, 494–509, https://doi.org/10.1037/0033-2909.114.3.494, 1993.

Collaud Coen, M., Andrews, E., Bigi, A., Martucci, G., Romanens, G., Vogt, F. P. A., and Vuilleumier, L.: Effects of the prewhitening method, the time granularity, and the time segmentation on the Mann–Kendall trend detection and the associated Sen's slope, Atmospheric Measurement Techniques, 13, 6945–6964, https://doi.org/10.5194/amt-13-6945-2020, 2020.

Dada, L., Paasonen, P., Nieminen, T., Buenrostro Mazon, S., Kontkanen, J., Peräkylä, O., Lehtipalo, K., Hussein, T., Petäjä, T., Kerminen, V.-M., Bäck, J., and Kulmala, M.: Long-term analysis of clear-sky new particle formation events and nonevents in Hyytiälä, Atmospheric Chemistry and Physics, 17, 6227–6241, https://doi.org/10.5194/acp-17-6227-2017, 2017.

Dal Maso, M., Kulmala, M., Riipinen, I., Wagner, R., Hussein, T., Aalto, P., and Lehtinen, K.: Formation and growth of fresh atmospheric aerosols: eight years of aerosol size distribution data from SMEAR II, Hyytiälä, Finland, Boreal Environment Research, 10, 323–336, https://www.borenv.net/BER/archive/pdfs/ber10/ber10-323.pdf, 2005.

Efron, B. and Tibshirani, R. J.: An Introduction to the Bootstrap, Chapman and Hall/CRC, 1 edn., https://doi.org/10.1201/9780429246593, 1994.

Hari, P. and Kulmala, M.: Station for Measuring Ecosystem–Atmosphere Relations (SMEAR II), Boreal Environment Research, 10, 315–322, https://www.borenv.net/BER/archive/pdfs/ber10/ber10-315.pdf, 2005.

Heikkinen, L., Äijälä, M., Riva, M., Luoma, K., Dällenbach, K., Aalto, J., Aalto, P., Aliaga, D., Aurela, M., Keskinen, H., Makkonen, U., Rantala, P., Kulmala, M., Petäjä, T., Worsnop, D., and Ehn, M.: Long-term sub-micrometer aerosol chemical composition in the boreal forest: inter- and intra-annual variability, Atmospheric Chemistry and Physics, 20, 3151–3180, https://doi.org/10.5194/acp-20-3151-2020, 2020.

https://doi.org/10.5194/egusphere-2026-3400
Preprint. Discussion started: 1 July 2026

Hendrickson, B. N., Alsante, A. N., and Brooks, S. D.: Live oak pollen as a source of atmospheric particles, Aerobiologia, 39, 51–67, https://doi.org/10.1007/s10453-022-09773-4, 2023.

Künsch, H. R.: The jackknife and the bootstrap for general stationary observations, The Annals of Statistics, 17, 1217–1241, https://doi.org/10.1214/aos/1176347265, 1989.

Luoma, K., Virkkula, A., Aalto, P., Petäjä, T., and Kulmala, M.: Over a 10-year record of aerosol optical properties at SMEAR II, Atmospheric Chemistry and Physics, 19, 11 363–11 382, https://doi.org/10.5194/acp-19-11363-2019, 2019.

Mann, H. B. and Whitney, D. R.: On a Test of Whether One of Two Random Variables Is Stochastically Larger than the Other, Annals of Mathematical Statistics, 18, 50–60, https://doi.org/10.1214/aoms/1177730491, 1947.

Meinander, O., Kouznetsov, R., Uppstu, A., Sofiev, M., Kaakinen, A., Salminen, J., Rontu, L., Welti, A., Francis, D., Piedehierro, A. A., Heikkilä, P., Heikkinen, E., and Laaksonen, A.: African dust transport and deposition modelling verified through a citizen science campaign in Finland, Scientific Reports, 13, https://doi.org/10.1038/s41598-023-46321-7, 2023.

Nie, W., Ding, A., Wang, T., Kerminen, V.-M., George, C., Xue, L., Wang, W., Zhang, Q., Petäjä, T., Qi, X., Gao, X., Wang, X., Yang, X., Fu, C., and Kulmala, M.: Polluted dust promotes new particle formation and growth, Scientific Reports, 4, https://doi.org/10.1038/srep06634, 2014.

Sarafian, R., Nissenbaum, D., Raveh-Rubin, S., Agrawal, V., and Rudich, Y.: Deep multi-task learning for early warnings of dust events implemented for the Middle East, npj Climate and Atmospheric Science, 6, 23, https://doi.org/10.1038/s41612-023-00348-9, 2023.

Schuster, G. L., Dubovik, O., and Holben, B. N.: Angstrom exponent and bimodal aerosol size distributions, Journal of Geophysical Research: Atmospheres, 111, https://doi.org/10.1029/2005jd006328, 2006.

Seinfeld, J. H. and Pandis, S. N.: Atmospheric Chemistry and Physics: From Air Pollution to Climate Change, John Wiley & Sons, Hoboken, NJ, 3 edn., 2016.

Steiner, A. L., Brooks, S. D., Deng, C., Thornton, D. C. O., Pendleton, M. W., and Bryant, V.: Pollen as atmospheric cloud condensation nuclei, Geophysical Research Letters, 42, 3596–3602, https://doi.org/10.1002/2015gl064060, 2015.

Titos, G., Burgos, M. A., Zieger, P., Alados-Arboledas, L., Baltensperger, U., Jefferson, A., Sherman, J., Weingartner, E., Henzing, B., Luoma, K., O'Dowd, C., Wiedensohler, A., and Andrews, E.: A global study of hygroscopicity-driven light-scattering enhancement in the context of other in situ aerosol optical properties, Atmospheric Chemistry and Physics, 21, 13 031–13 050, https://doi.org/10.5194/acp-21-13031-2021, 2021.

Tuel, A. and Martius, O.: A climatology of sub-seasonal temporal clustering of extreme precipitation in Switzerland and its links to extreme discharge, Natural Hazards and Earth System Sciences, 21, 2949–2972, https://doi.org/10.5194/nhess-21-2949-2021, 2021.

Varga, G., Meinander, O., Rostási, Á., Dagsson-Waldhauserova, P., Csávics, A., and Gresina, F.: Saharan, Aral-Caspian and Middle East dust travels to Finland (1980–2022), Environment International, 180, 108 243, https://doi.org/10.1016/j.envint.2023.108243, 2023.

Vargha, A. and Delaney, H. D.: A Critique and Improvement of the CL Common Language Effect Size Statistics of McGraw and Wong, Journal of Educational and Behavioral Statistics, 25, 101–132, https://doi.org/10.3102/10769986025002101, 2000.

Wiedensohler, A., Birmili, W., Nowak, A., Sonntag, A., Weinhold, K., Merkel, M., Wehner, B., Tuch, T., Pfeifer, S., Fiebig, M., Fjäraa, A. M., Asmi, E., Sellegri, K., Depuy, R., Venzac, H., Villani, P., Laj, P., Aalto, P., Ogren, J. A., Swietlicki, E., Williams, P., Roldin, P., Quincey, P., Hüglin, C., Fierz-Schmidhauser, R., Gysel, M., Weingartner, E., Riccobono, F., Santos, S., Grüning, C., Faloon, K., Beddows, D., Harrison, R., Monahan, C., Jennings, S. G., O'Dowd, C. D., Marinoni, A., Horn, H.-G., Keck, L., Jiang, J., Scheckman, J., McMurry, P. H., Deng, Z., Zhao, C. S., Moerman, M., Henzing, B., de Leeuw, G., Löschau, G., and Bastian, S.: Mobility particle size spectrometers:

https://doi.org/10.5194/egusphere-2026-3400
Preprint. Discussion started: 1 July 2026

harmonization of technical standards and data structure to facilitate high quality long-term observations of atmospheric particle number size distributions, Atmospheric Measurement Techniques, 5, 657–685, https://doi.org/10.5194/amt-5-657-2012, 2012.